# ROBUST MULTIVARIATE PROCESS MONITORING USING SVM AND PROBABILITY OF CONTROL

Mohammed Moyed Ahmed[1]

*Multivariate statistical process control (MSPC) is crucial for maintaining product quality and process efficiency in modern manufacturing. However, traditional MSPC methods often struggle with two key challenges: detecting small shifts in process parameters and identifying the variables responsible for these shifts, particularly in non-normal and highly correlated processes. This study proposes a novel approach to address these limitations using Support Vector Machines (SVM) and a Probability of Control (PoC) concept. Our method, termed SVM-PoC, integrates the classification power of SVM with a probabilistic framework to create a robust control chart for multivariate processes. Unlike traditional approaches, SVM-PoC does not rely on normality assumptions and remains effective across various correlation structures. The method not only detects process shifts but also identifies the source variables causing these shifts. Through extensive simulation studies, we evaluated the performance of SVM-PoC in both normal and non-normal (gamma-distributed) processes under various shift magnitudes and correlation levels. Results demonstrate that SVM-PoC consistently outperforms traditional methods like Hotelling's* $T^2$ *chart, especially in detecting small shifts and in non-normal scenarios. Moreover, it accurately identifies shift sources even in highly correlated processes, a significant advancement over existing techniques. The proposed method's flexibility and accuracy make it particularly relevant for industries dealing with complex, multivariate processes where traditional assumptions may not hold. By providing a unified approach for shift detection and source identification across various process conditions, SVM-PoC offers a valuable tool for enhancing process monitoring and quality improvement efforts in modern manufacturing environments. This research contributes to the field of MSPC by offering a novel, data-driven approach that addresses longstanding challenges in multivariate process monitoring, potentially improving process control strategies across diverse industrial applications*

**Keywords:** Multivariate Statistical Process Control (MSPC), Support Vector Machines (SVM), Probability of Control (PoC), Non-normal Distribution, Gamma Distribution, Machine Learning.

---

[1] ECE, Department, JNTUH, Hyderabad, India, e-mail: mmoyed@gmail.com

## 1. **Introduction**

Statistical process control (SPC) is a fundamental approach in quality management, playing a crucial role in maintaining product quality and process stability across various industries. In modern manufacturing and service processes, the complexity of operations often necessitates the simultaneous monitoring of multiple quality variables, giving rise to the field of multivariate statistical process control (MSPC) [1], [2]. Traditional SPC approaches, which monitor each variable independently, have been found inadequate in scenarios where quality variables exhibit significant correlations. This limitation has driven the development of MSPC techniques that consider the joint probability distribution of quality variables, thereby providing a more accurate representation of the process state [3].

The primary objectives of MSPC are twofold: first, to detect shifts in the process that indicate an out-of-control situation, and second, to identify the specific variable(s) responsible for such shifts. These objectives are critical for maintaining process efficiency, reducing waste, and ensuring consistent product quality. However, achieving these goals in multivariate settings presents significant challenges, particularly as the number of monitored variables increases [4]. Numerous studies have addressed these challenges, proposing various methods for multivariate process monitoring. However, many existing methods suffer from limitations such as the assumption of normality, sensitivity to correlation structures, and computational complexity [5].

These constraints can lead to suboptimal performance in real-world scenarios where processes may exhibit non-normal distributions or complex variable interactions. In recent years, there has been growing interest in leveraging machine learning techniques to overcome the limitations of traditional MSPC methods. Among these, Support Vector Machines (SVM) have shown particular promise due to their ability to handle high-dimensional data and non-linear relationships without making strong distributional assumptions[6].

This study proposes a novel data-based method utilizing Support Vector Machines (SVM) to address the challenges in multivariate process monitoring. Our approach aims to overcome the limitations of traditional model-based methods by offering a flexible, distribution-free solution capable of both detecting shifts and identifying their sources in multivariate processes. By integrating the strengths of SVM with the principles of MSPC, we seek to develop a robust tool that can effectively monitor complex processes across various industries.

The remainder of this paper is organized as follows: Section 2 provides a comprehensive review of related work in MSPC and machine learning applications in process control. Section 3 presents the theoretical framework of our proposed SVM-based approach. Section 4 details the simulation study conducted to evaluate the performance of the method. Section 5 discusses the experimental findings and their implications. Finally, Section 6 concludes the study and suggests directions for future research.

## 2. **Related work**

The field of Multivariate Statistical Process Control (MSPC) has evolved significantly over the past decades, driven by the increasing complexity of manufacturing processes and the need for more sophisticated monitoring techniques. This section provides an overview of the key developments in MSPC and the recent integration of machine learning approaches.

The foundation of MSPC was laid by Hotelling with the introduction of the $T^2$ statistic, which formed the basis for Shewhart-type multivariate control charts. While widely used, Hotelling's $T^2$ was found to be less effective in detecting small shifts in the process mean vector [7]. This limitation led to the development of more sensitive techniques such as the Multivariate Cumulative Sum (MCUSUM) by Crosier and the Multivariate Exponential Weighted Moving Average (MEWMA) by Lowry et al. [8]. These methods improved shift detection by incorporating information from previous samples. However, these traditional approaches often rely on the assumption of multivariate normality, which may not hold in many real-world scenarios. To address this, researchers have proposed various methods for non-normal processes. For instance, Liu developed a method capable of simultaneously detecting shifts in both mean and variance for non-normal processes. Chang and Bai proposed an adaptation of Hotelling's $T^2$ for skewed distributions using weighted standard deviations [9].

The application of advanced analytics and machine learning techniques to process monitoring and fault diagnosis has gained significant attention in recent years. A growing body of research explores the use of these techniques to improve the efficiency and effectiveness of industrial processes. One area of research focuses on the development of novel methods for recognizing control chart patterns, which are critical for quality control in manufacturing by Khormali and Addeh [10]. Another stream of research investigates the application of machine learning techniques to statistical process monitoring, including classification, clustering, and regression by Yu in the year 2022. These studies demonstrate the potential of machine learning to improve the accuracy and efficiency of process monitoring.

Data-driven approaches to root cause diagnosis have also been explored, showcasing the effectiveness of machine learning and analytics techniques in identifying the underlying causes of process faults in 2022 by Jiang et al [11]. Furthermore, Yao and Gao conducted the reviews of multistage process monitoring methods, highlighting the complexity and variability inherent in these systems [12]. The integration of data analytics and machine learning in smart manufacturing has been extensively researched, with a focus on applications and perspectives by Shang et al. in 2023 [13]. Additionally, reviews of process monitoring and fault diagnosis in specific industries, such as wind turbines, have been conducted by Wu et al., showcasing the potential of advanced analytics techniques in these areas [14].

Recent research has also focused on the development of novel methods for fault classification and detection, including the application of convolutional neural networks (CNNs) to gearbox and rotating machinery faults Liao et al., in 2023; Janssens et al., in 2023 [15],[16]. These studies demonstrate the effectiveness of deep learning techniques in identifying complex patterns in process data. Finally, reviews of data-based process monitoring have been conducted by Ge et al., highlighting recent advances in techniques for monitoring, fault detection, and diagnosis [17]. These studies demonstrate the rapidly evolving landscape of process monitoring and fault diagnosis, and the growing importance of advanced analytics and machine learning techniques in this field. Recent research has focused on addressing the dual challenge of shift detection and source identification. Bisheh and Amiri [18] proposed a method combining kernel PCA with a variable-wise decomposition algorithm, using SVM as a decision-making tool for feature selection. This approach demonstrated accuracy in identifying slippage under changing conditions.

Despite these advancements, many existing methods still face challenges in simultaneously addressing shift detection and source identification, particularly in the context of non-normal distributions and correlated variables. Additionally, sensitivity to the magnitude of process shifts remains a concern for many techniques [19]. The proposed method aims to build upon these developments, leveraging the strengths of SVM to create a comprehensive MSPC tool that can both detect shifts and identify their sources, while remaining robust to non-normal distributions, correlated variables, and varying shift magnitudes. By addressing these gaps, we seek to contribute to the ongoing evolution of MSPC techniques and their practical application in complex industrial processes.

## 3. SVM (SUPPORT VECTOR MACHINE) OVERVIEW

Support Vector Machine (SVM) is a powerful machine learning algorithm initially developed to address binary classification problems. Since its inception, SVM has found widespread application in various fields, including decision-making, text categorization, digital image analysis, character identification, and bioinformatics. The fundamental principle behind SVM lies in its ability to utilize geometric features to obtain an optimal hyperplane by solving a convex optimization problem. This process simultaneously minimizes the generalization error and maximizes the geometric margin between classes [20]. The mathematical framework of SVM can be described as follows:

Given a training dataset $(x_i, y_i)$, where $i = 1, 2, \ldots, N$, where $y \in \{-1, 1\}$ represents the binary class labels, and $z$ being a test data point, the SVM decision function is defined as:

$$f(z) = \sum_{i=1}^{N} \alpha_i y_i K(x_i, z) + b \tag{1}$$

Where:

- $\alpha_i$ are Lagrange multipliers obtained through quadratic programming under cost constraints.
- $K(x_j, x_i)$ is the kernel function.
- $b$ is a model parameter.

The parameter $b$ is determined by solving the following equation:

$$\alpha_i \left\{ y_i \left( \sum_{j=1}^{N} \alpha_j y_j K(x_j, x_i) + b \right) - 1 \right\} = 0 \tag{2}$$

In many applications, the radial basis function (RBF) is chosen as the kernel, defined as:

$$K(x_i, x_j) = \exp(-\gamma \|x_i - x_j\|^2) \tag{3}$$

Where $\gamma$ is a kernel parameter that controls the width of the Gaussian function.

While SVM is inherently a binary classifier, it can be extended to provide probabilistic outputs, which are particularly useful in process control applications. Platt proposed a method to obtain classification probabilities from the SVM model by training an additional sigmoid function on the SVM outputs.

The probability estimation, known as Probability of Control (PoC), for a test data point $z_i$ is given by:

$$PoC_i = \frac{1}{1 + \exp(Af(z_i) + B)} \tag{4}$$

Where $A$ and $B$ are parameters of the sigmoid function, obtained by solving an optimization problem on the training data [20].

In the context of process control, Chongfuangprinya et al,. demonstrated the effectiveness of using SVM-PoC values for classification in both normal and abnormal process conditions. They established a threshold value of 0.50, above which a process is considered to be in control. The SVM-PoC approach offers several advantages in multivariate process control:

1. Non-linear decision boundaries: SVM can effectively handle non-linear relationships between variables through the use of kernel functions.

2. Robustness to high-dimensional data: SVM performs well even when the number of features is large relative to the number of observations.

3. Probabilistic output: The PoC provides a continuous measure of the process state, allowing for more nuanced monitoring than binary classifications.

4. Flexibility: SVM does not require strong assumptions about the underlying data distribution, making it suitable for a wide range of process conditions.

These characteristics make SVM a promising tool for addressing the challenges in multivariate statistical process control, particularly in situations where traditional methods may fall short due to non-normality or complex variable interactions.

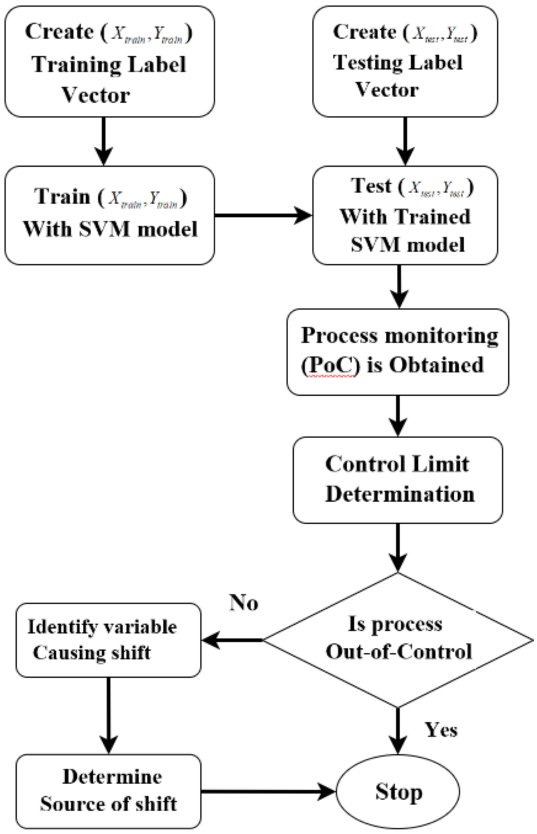


FIG. 1. The Proposed Framework

## 4. **Proposed Method**

In this study, Probability of Correct classification (PoC) control charts inspired by Chongfuangprinya et al. [20] were created to detect and describe shifts in a multivariate process. However, unlike the referenced study, the probability of misclassification was used as a process monitoring statistic for ease of calculation. Typically, when the probability distribution of the monitoring statistic is known, control limits for the control chart can be obtained based on a specified Type I error rate. Since the distribution of monitoring statistics in the PoC control chart is unknown, the control limit is determined

**Algorithm 3.1** Multivariable Process Monitoring using DVM

```
Collect datasets $\mathcal{X}_{\text{control}}$ and $\mathcal{X}_{\text{out\_of\_control}}$
Combine datasets to create a complete training dataset $\mathcal{X}_{\text{train}}$
Create corresponding label vector $\mathbf{y}_{\text{train}}$
    ▷ $\mathbf{y}_{\text{train}} = \begin{cases} +1, & \text{if } i \in \mathcal{X}_{\text{control}} \\ -1, & \text{if } i \in \mathcal{X}_{\text{out\_of\_control}} \end{cases}$
Train DVM model using the training data $(\mathcal{X}_{\text{train}}, \mathbf{y}_{\text{train}})$
    ▷ Model learns normal behavior of the process based on control data
Generate new test dataset $\mathcal{X}_{\text{test}}$ similar to the training data $\mathcal{X}_{\text{train}}$
Label test data $\mathcal{X}_{\text{test}}$ with the corresponding vector $\mathbf{y}_{\text{test}}$
Test trained DVM model on the test dataset $\mathcal{X}_{\text{test}}$
Calculate classification probabilities for each observation in $\mathcal{X}_{\text{test}}$
Identify classification probabilities for observations in $\mathcal{X}_{\text{test}}$ that were labeled as out of control
Determine the average classification probability for these out-of-control observations (Process Out-of-Control (PoC) statistic)
Calculate 99th percentile of PoC statistic using the bootstrap method
    ▷ 99th percentile represents the control limit for the process
Compare actual PoC statistic with control limit
    ▷ If PoC statistic exceeds control limit, indicate that the process is likely out of control
```

using the bootstrap method. Bootstrap is a widely used resampling method for statistical estimation when the underlying distribution is unknown.

In the PoC control chart, process monitoring statistics are tracked against this bootstrapped control limit. If the process monitoring statistics exceed the control limit, the process is deemed out of control; otherwise, it is considered under control. This approach determines whether there is a shift in the process. The proposed method uses classification probabilities corresponding to ”-1” (out-of-control) or ”+1” (in-control) labels to describe the process state. The matrix of classification probabilities serves as the tracking statistic. Specifically, the averages of the misclassification probabilities corresponding to ”+1” were used. In other words, the average probability that an in-control process is classified as out-of-control serves as the monitoring statistic for the control chart.

The rationale for using mean classification probabilities to monitor process drift is that these average values reflect overall changes in the process. By comparing these values to the control limits, we can determine whether the process remains in control. After detecting an out-of-control state, the study also identified which variable(s) caused the shift by examining the combination of changes corresponding to the largest average value in the classification probability matrix.

The algorithmic steps of the DVM-based multivariate process monitoring procedure conducted in this study are as follows: Algorithm for Multivariable Process Monitoring using DVM, this algorithm describes the steps involved in monitoring a multivariable process using a Dynamic Vector Machine (DVM) model. The goal is to identify when the process deviates from its normal operating conditions.

As shown in the **Figure** 1 and **Algorithm 4.1**, illustrates algorithm steps for Multivariable Process Monitoring using DVM, in this study:

**Step 1:** Data Collection and Preparation, Collect a dataset of $n_1$ observations under normal operating conditions (control data) and $n_2$ observations when the process is out of control (out-of-control data). Combine the control and out-of-control data to create a complete training dataset with $N = n_1 + n_2$ observations. Create a corresponding label vector with values of $+1$ for observations under control and $-1$ for observations out of control.

**Step 2:** DVM Model Training, Train the DVM model using the training data $(X_{\text{train}}, Y_{\text{train}})$. The model learns the normal behavior of the process based on the control data.

**Step 3:** Test Data Generation, Generate a new test dataset similar to the training data.

**Step 4:** Test Data Labeling, Label the test data with corresponding values of $+1$ for observations under control and $-1$ for observations out of control.

**Step 5:** DVM Model Testing and Probability Calculation, Test the trained DVM model on the test dataset and calculate classification probabilities for each observation in the test dataset.

**Step 6:** Process Out-of-Control Detection, Identify the classification probabilities for observations labeled as out of control and calculate the average classification probability. This value is known as the Process Out-of-Control (PoC) statistic.

**Step 7:** Control Limit Determination, Use the bootstrap method to calculate the 99th percentile of the PoC statistic. This value represents the control limit for the process.

**Step 8:** Out-of-Control Decision, Compare the actual PoC statistic with the control limit. If the actual PoC statistic exceeds the control limit, the process is determined to be out of control.

**Step 9:** Identifying Contributing Factors (if out of control), If the process is determined to be out of control, identify the combination of observations that yields the highest average PoC statistic as the likely cause of the process deviation.

The above methodology provides a structured approach for monitoring multivariable processes using a DVM model and identifying contributing factors to process deviations.

## 5. **Simulation Details**

All analyses were performed using MATLAB (2022b). 10,000 replications were used to calculate ARL values for performance comparisons, 2,000 replications were used for source identification simulations. This comprehensive simulation study allows us to evaluate the proposed method's effectiveness in shift detection and source identification across a wide range of process conditions, including both normal and non-normal multivariate processes with varying degrees of correlation and shift magnitudes.

TABLE 1. ARL values obtained using the Probability of Control chart in a process that follows a multivariate normal distribution. $(\mu_0 + \delta\sigma, \Sigma_0)$

| $\delta\sigma$ | $\rho_3 = 0.8$ | $\rho_2 = 0.5$ | $\rho_1 = 0.3$ |
|---|---|---|---|
| 0.00 | 97.77 | 97.85 | 98.48 |
| 0.25 | 5.88 | 5.57 | 5.47 |
| 0.50 | 5.59 | 5.35 | 4.22 |
| 0.75 | 4.71 | 4.43 | 3.81 |
| 1.00 | 4.25 | 3.97 | 3.28 |
| 1.50 | 2.91 | 2.41 | 2.04 |
| 2.00 | 1.79 | 1.55 | 1.26 |
| 2.50 | 1.34 | 1.15 | 1.06 |
| 3.00 | 1.10 | 1.03 | 1.01 |

### **Multivariate Normal Distribution Processes**

*i. Shift Detection Performance.* The results in Table 1 demonstrate the effectiveness of the Probability of Control (PoC) chart based on the SVM approach across various correlation levels ($\rho_1 = 0.3$, $\rho_2 = 0.5$, and $\rho_3 = 0.8$) and shift magnitudes ($\delta$).

When examining the in-control performance ($\delta = 0$), the ARL values (97.77, 97.85, and 98.48) are very close to the target $ARL_0$ of 100, indicating proper calibration of the control chart. This slight deviation is within acceptable statistical error given the 10,000 replications used in the simulations.

Table 2. ARL values derived from the $T^2$ and Probability of Control charts in a process adhering to a multivariate normal distribution. $(\mu_0 + \delta\sigma; \Sigma_0)$

| $\delta\sigma$ | $\rho_3 = 0.8$ | | $\rho_2 = 0.5$ | | $\rho_1 = 0.3$ | |
|---|---|---|---|---|---|---|
| | $T^2$ | PoC | $T^2$ | PoC | $T^2$ | PoC |
| 0.00 | 100.78 | 97.77 | 100.14 | 97.85 | 99.46 | 98.48 |
| 0.25 | 89.76 | 5.88 | 86.25 | 5.57 | 82.27 | 5.47 |
| 0.50 | 64.05 | 5.59 | 58.93 | 5.35 | 52.26 | 4.22 |
| 0.75 | 42.14 | 4.71 | 34.93 | 4.43 | 28.86 | 3.81 |
| 1.00 | 27.05 | 4.25 | 20.48 | 3.97 | 16.30 | 3.28 |
| 1.50 | 10.76 | 2.91 | 7.70 | 2.41 | 5.69 | 2.04 |
| 2.00 | 5.03 | 1.79 | 3.43 | 1.55 | 2.62 | 1.26 |
| 2.50 | 2.74 | 1.34 | 1.97 | 1.15 | 1.57 | 1.06 |
| 3.00 | 1.78 | 1.10 | 1.38 | 1.03 | 1.18 | 1.01 |

Table 3. ARL values derived from the Probability of control chart in processes that follow a multivariate Gamma distribution.

| $\delta$ | Gamma 1 $(\theta_1 + \delta\sigma; \theta_2)$ | | | Gamma 2 $(\theta_1; \theta_2 + \delta)$ | | | Gamma 3 $(\theta_1 + \delta; \theta_2)$ | | |
|---|---|---|---|---|---|---|---|---|---|
| | $\rho_3 = 0.8$ | $\rho_2 = 0.5$ | $\rho_1 = 0.3$ | $\rho_3 = 0.8$ | $\rho_2 = 0.5$ | $\rho_1 = 0.3$ | $\rho_3 = 0.8$ | $\rho_2 = 0.5$ | $\rho_1 = 0.3$ |
| 0.00 | 98.76 | 99.83 | 99.83 | 99.97 | 98.77 | 97.56 | 99.07 | 100.13 | 98.96 |
| 0.25 | 5.78 | 2.44 | 1.88 | 2.02 | 1.60 | 1.50 | 1.33 | 1.37 | 1.53 |
| 0.50 | 1.68 | 1.46 | 1.36 | 1.60 | 1.49 | 1.48 | 1.11 | 1.13 | 1.18 |
| 0.75 | 1.57 | 1.26 | 1.22 | 1.54 | 1.45 | 1.42 | 1.02 | 1.05 | 1.05 |
| 1.00 | 1.25 | 1.11 | 1.05 | 1.50 | 1.38 | 1.38 | 1.01 | 1.01 | 1.01 |
| 1.50 | 1.11 | 1.03 | 1.01 | 1.28 | 1.23 | 1.23 | 1.00 | 1.00 | 1.00 |
| 2.00 | 1.03 | 1.02 | 1.01 | 1.28 | 1.25 | 1.23 | 1.01 | 1.00 | 1.00 |
| 2.50 | 1.02 | 1.01 | 1.01 | 1.24 | 1.17 | 1.15 | 1.00 | 1.00 | 1.00 |
| 3.00 | 1.01 | 1.00 | 1.00 | 1.22 | 1.16 | 1.12 | 1.00 | 1.00 | 1.00 |

For out-of-control scenarios, the PoC chart shows remarkable sensitivity to small shifts. At $\delta = 0.25\sigma$, the ARL values range from 5.47 to 5.88, indicating that the chart can detect such small shifts within approximately 5-6 samples. This sensitivity increases as shift magnitude increases, with ARL values dropping to approximately 1 for shifts of $3\sigma$.

Interestingly, the chart's performance improves slightly as correlation decreases (from $\rho_3 = 0.8$ to $\rho_1 = 0.3$). For example, at $\delta = 0.5\sigma$, the ARL decreases from 5.59 ($\rho_3 = 0.8$) to 4.22 ($\rho_1 = 0.3$). This suggests that the SVM approach efficiently handles the additional information provided by less correlated variables, unlike traditional methods where high correlation typically causes performance degradation.

*ii. Comparison with Hotelling's $T^2$ Control Chart.* Table 2 offers a direct comparison between the proposed PoC chart and the widely used Hotelling's

TABLE 4. 2. SVM-PoC (average values) according to different combinations of changes in a process that conforms to a multivariate normal distribution

| Normal Dağılım ($\boldsymbol{\mu}_0 + \delta\sigma; \boldsymbol{\Sigma}_0$) | | | | | | | | | | | | | | | | | | | | | | |
|---|---|---|---|---|---|---|---|---|---|---|---|---|---|---|---|---|---|---|---|---|---|---|
| | | $\rho_3 = 0{,}8$ | | | | | | | $\rho_2 = 0{,}5$ | | | | | | | $\rho_1 = 0{,}3$ | | | | | | |
| $\delta\sigma$ | | 1 | 2 | 3 | 4 | 5 | 6 | 7 | 1 | 2 | 3 | 4 | 5 | 6 | 7 | 1 | 2 | 3 | 4 | 5 | 6 | 7 |
| 0 | 0 | 2,000 | 2,000 | 2,000 | 2,000 | 2,000 | 2,000 | 2,000 | 2,000 | 2,000 | 2,000 | 2,000 | 2,000 | 2,000 | 2,000 | 2,000 | 2,000 | 2,000 | 2,000 | 2,000 | 2,000 | 2,000 |
| | 1 | 2,018 | 2,013 | 2,018 | 2,012 | 2,016 | 2,011 | 2,010 | 2,036 | 2,020 | 2,016 | 2,007 | 2,015 | 2,008 | 2,005 | 2,042 | 2,019 | 2,025 | 2,008 | 2,021 | 2,010 | 2,008 |
| | 2 | 2,012 | 2,165 | 2,001 | 2,063 | 2,001 | 2,041 | 2,014 | 2,010 | 2,061 | 2,004 | 2,019 | 2,002 | 2,015 | 2,004 | 2,024 | 2,044 | 2,004 | 2,010 | 2,005 | 2,008 | 2,001 |
| | 3 | 2,009 | 2,002 | 2,217 | 2,057 | 2,003 | 2,020 | 2,049 | 2,015 | 2,002 | 2,057 | 2,023 | 2,003 | 2,013 | 2,014 | 2,020 | 2,005 | 2,049 | 2,012 | 2,006 | 2,003 | 2,020 |
| 0,5 | 4 | 2,003 | 2,051 | 2,065 | 2,179 | 2,019 | 2,004 | 2,005 | 2,006 | 2,013 | 2,012 | 2,028 | 2,004 | 2,002 | 2,002 | 2,007 | 2,009 | 2,009 | 2,016 | 2,001 | 2,001 | 2,002 |
| | 5 | 2,011 | 2,001 | 2,002 | 2,016 | 2,204 | 2,049 | 2,057 | 2,024 | 2,001 | 2,002 | 2,004 | 2,069 | 2,015 | 2,015 | 2,023 | 2,004 | 2,005 | 2,002 | 2,038 | 2,011 | 2,014 |
| | 6 | 2,008 | 2,054 | 2,011 | 2,003 | 2,046 | 2,157 | 2,004 | 2,004 | 2,011 | 2,003 | 2,003 | 2,020 | 2,033 | 2,002 | 2,011 | 2,011 | 2,003 | 2,002 | 2,016 | 2,013 | 2,002 |
| | 7 | 2,005 | 2,011 | 2,056 | 2,004 | 2,048 | 2,005 | 2,164 | 2,007 | 2,007 | 2,017 | 2,002 | 2,014 | 2,003 | 2,029 | 2,009 | 2,003 | 2,014 | 2,001 | 2,014 | 2,002 | 2,017 |
| | 1 | 2,291 | 2,152 | 2,157 | 2,076 | 2,158 | 2,069 | 2,084 | 2,446 | 2,220 | 2,183 | 2,063 | 2,167 | 2,065 | 2,056 | 2,587 | 2,283 | 2,250 | 2,064 | 2,253 | 2,087 | 2,074 |
| | 2 | 2,083 | 4,402 | 2,066 | 2,620 | 2,073 | 2,595 | 2,027 | 2,192 | 2,820 | 2,027 | 2,199 | 2,023 | 2,193 | 2,002 | 2,284 | 2,650 | 2,047 | 2,165 | 2,046 | 2,141 | 2,003 |
| | 3 | 2,098 | 2,059 | 4,459 | 2,543 | 2,065 | 2,021 | 2,576 | 2,192 | 2,031 | 2,784 | 2,175 | 2,020 | 2,003 | 2,162 | 2,304 | 2,046 | 2,649 | 2,147 | 2,050 | 2,003 | 2,173 |
| 1,0 | 4 | 2,044 | 2,572 | 2,548 | 4,043 | 2,033 | 2,033 | 2,031 | 2,063 | 2,198 | 2,203 | 2,487 | 2,002 | 2,002 | 2,002 | 2,092 | 2,162 | 2,196 | 2,294 | 2,001 | 2,001 | 2,003 |
| | 5 | 2,098 | 2,062 | 2,060 | 2,021 | 4,371 | 2,567 | 2,548 | 2,189 | 2,022 | 2,020 | 2,005 | 2,734 | 2,163 | 2,169 | 2,317 | 2,046 | 2,062 | 2,002 | 2,676 | 2,156 | 2,159 |
| | 6 | 2,037 | 2,577 | 2,032 | 2,036 | 2,586 | 4,062 | 2,033 | 2,075 | 2,212 | 2,001 | 2,002 | 2,216 | 2,498 | 2,002 | 2,092 | 2,195 | 2,002 | 2,001 | 2,185 | 2,296 | 2,001 |
| | 7 | 2,037 | 2,027 | 2,533 | 2,030 | 2,602 | 2,026 | 4,106 | 2,061 | 2,002 | 2,166 | 2,002 | 2,193 | 2,002 | 2,398 | 2,099 | 2,002 | 2,166 | 2,002 | 2,166 | 2,001 | 2,241 |
| | 1 | 3,336 | 2,550 | 2,513 | 2,341 | 2,539 | 2,345 | 2,302 | 4,081 | 2,835 | 2,841 | 2,254 | 2,834 | 2,281 | 2,281 | 4,897 | 3,137 | 3,115 | 2,313 | 3,152 | 2,306 | 2,326 |
| | 2 | 2,275 | 7,470 | 3,126 | 3,988 | 3,137 | 3,934 | 2,838 | 2,742 | 5,015 | 2,186 | 2,675 | 2,183 | 2,735 | 2,033 | 3,182 | 4,561 | 2,254 | 2,637 | 2,229 | 2,559 | 2,016 |
| | 3 | 2,300 | 3,115 | 7,424 | 3,887 | 3,190 | 2,830 | 4,043 | 2,768 | 2,175 | 5,009 | 2,728 | 2,193 | 2,038 | 2,721 | 3,233 | 2,279 | 4,614 | 2,593 | 2,256 | 2,015 | 2,605 |
| 1,5 | 4 | 2,185 | 4,322 | 4,195 | 6,979 | 3,089 | 2,930 | 2,848 | 2,271 | 2,748 | 2,714 | 3,835 | 2,060 | 2,037 | 2,025 | 2,376 | 2,654 | 2,626 | 3,288 | 2,037 | 2,020 | 2,018 |
| | 5 | 2,270 | 3,174 | 3,069 | 2,850 | 7,361 | 3,932 | 4,024 | 2,762 | 2,172 | 2,187 | 2,033 | 4,973 | 2,744 | 2,731 | 3,147 | 2,274 | 2,266 | 2,021 | 4,405 | 2,528 | 2,587 |
| | 6 | 2,157 | 4,141 | 3,034 | 2,810 | 4,214 | 6,914 | 2,841 | 2,264 | 2,743 | 2,059 | 2,031 | 2,752 | 3,935 | 2,028 | 2,398 | 2,735 | 2,031 | 2,017 | 2,739 | 3,381 | 2,013 |
| | 7 | 2,149 | 3,004 | 4,131 | 2,837 | 4,152 | 2,984 | 6,995 | 2,272 | 2,063 | 2,846 | 2,036 | 2,792 | 2,032 | 4,079 | 2,364 | 2,038 | 2,672 | 2,016 | 2,633 | 2,015 | 3,350 |
| | 1 | 5,183 | 3,540 | 3,506 | 3,267 | 3,488 | 3,393 | 3,208 | 6,167 | 3,854 | 4,099 | 2,736 | 3,821 | 2,701 | 2,726 | 6,885 | 4,602 | 4,494 | 2,712 | 4,435 | 2,694 | 2,723 |
| | 2 | 2,766 | 9,049 | 6,373 | 6,336 | 6,455 | 6,453 | 6,085 | 3,631 | 7,253 | 2,928 | 3,490 | 2,869 | 3,665 | 2,331 | 4,588 | 6,815 | 2,827 | 3,332 | 2,806 | 3,350 | 2,134 |
| | 3 | 2,670 | 6,313 | 9,079 | 6,461 | 6,426 | 5,965 | 6,221 | 3,596 | 2,994 | 7,240 | 3,581 | 2,920 | 2,359 | 3,638 | 4,420 | 2,859 | 6,793 | 3,327 | 2,835 | 2,155 | 3,343 |
| 2,0 | 4 | 2,643 | 6,801 | 6,882 | 8,783 | 6,348 | 5,886 | 5,912 | 2,867 | 3,910 | 3,868 | 5,963 | 2,608 | 2,283 | 2,287 | 3,058 | 3,614 | 3,642 | 5,082 | 2,333 | 2,127 | 2,131 |
| | 5 | 2,700 | 6,167 | 6,184 | 5,806 | 9,126 | 6,233 | 6,279 | 3,661 | 3,033 | 3,050 | 2,405 | 7,104 | 3,506 | 3,577 | 4,459 | 2,819 | 2,781 | 2,163 | 6,788 | 3,324 | 3,339 |
| | 6 | 2,608 | 6,823 | 6,493 | 5,767 | 6,594 | 8,837 | 5,779 | 2,836 | 3,858 | 2,584 | 2,286 | 3,991 | 5,998 | 2,335 | 3,096 | 3,544 | 2,340 | 2,141 | 3,620 | 5,046 | 2,155 |
| | 7 | 2,735 | 6,393 | 6,995 | 6,085 | 6,910 | 5,937 | 8,807 | 2,807 | 2,589 | 3,903 | 2,325 | 3,872 | 2,332 | 6,177 | 2,977 | 2,310 | 3,601 | 2,120 | 3,662 | 2,106 | 5,193 |
| | 1 | 6,960 | 5,616 | 5,695 | 5,236 | 5,829 | 5,259 | 5,237 | 7,728 | 5,783 | 5,661 | 3,855 | 5,732 | 3,915 | 3,825 | 8,542 | 5,758 | 6,040 | 3,290 | 5,837 | 3,267 | 3,352 |
| | 2 | 3,615 | 9,764 | 8,677 | 8,401 | 8,603 | 8,348 | 8,330 | 5,062 | 8,614 | 5,053 | 4,853 | 5,052 | 4,847 | 3,750 | 6,278 | 8,226 | 4,655 | 4,366 | 4,588 | 4,353 | 3,019 |
| | 3 | 3,457 | 8,602 | 9,715 | 8,309 | 8,608 | 8,363 | 8,503 | 4,970 | 5,046 | 8,614 | 4,886 | 5,068 | 3,849 | 4,990 | 6,236 | 4,583 | 8,267 | 4,293 | 4,649 | 2,839 | 4,335 |
| 2,5 | 4 | 3,966 | 8,851 | 8,826 | 9,604 | 8,607 | 8,485 | 8,428 | 4,117 | 5,639 | 5,643 | 7,678 | 4,517 | 3,612 | 3,690 | 4,491 | 5,111 | 5,033 | 6,898 | 3,674 | 2,685 | 2,683 |
| | 5 | 3,314 | 8,658 | 8,546 | 8,283 | 9,737 | 8,437 | 8,383 | 5,179 | 5,270 | 5,106 | 3,976 | 8,586 | 4,855 | 5,000 | 6,286 | 4,652 | 4,519 | 2,834 | 8,291 | 4,220 | 4,360 |
| | 6 | 4,032 | 8,811 | 8,722 | 8,411 | 8,831 | 9,622 | 8,262 | 4,065 | 5,536 | 4,663 | 3,674 | 5,524 | 7,688 | 3,665 | 4,395 | 5,038 | 3,653 | 2,611 | 4,909 | 6,734 | 2,687 |
| | 7 | 4,062 | 8,623 | 8,755 | 8,378 | 8,681 | 8,376 | 9,584 | 4,221 | 4,748 | 5,805 | 3,755 | 5,830 | 3,729 | 7,723 | 4,320 | 3,743 | 5,086 | 2,688 | 4,829 | 2,600 | 6,694 |
| | 1 | 8,166 | 7,525 | 7,549 | 7,172 | 7,505 | 7,292 | 7,377 | 8,842 | 7,427 | 7,314 | 5,262 | 7,317 | 5,594 | 5,432 | 9,291 | 7,377 | 7,697 | 4,697 | 7,326 | 4,376 | 4,308 |
| | 2 | 4,648 | 9,938 | 9,529 | 9,443 | 9,588 | 9,436 | 9,471 | 6,422 | 9,401 | 7,069 | 6,424 | 6,957 | 6,032 | 5,882 | 7,967 | 9,176 | 6,813 | 5,475 | 6,715 | 5,634 | 4,690 |
| | 3 | 4,853 | 9,602 | 9,935 | 9,412 | 9,594 | 9,506 | 9,406 | 6,615 | 7,181 | 9,383 | 6,354 | 7,318 | 6,007 | 6,246 | 7,579 | 6,574 | 9,231 | 5,477 | 6,258 | 4,463 | 5,365 |
| 3,0 | 4 | 5,692 | 9,653 | 9,668 | 9,898 | 9,561 | 9,491 | 9,467 | 6,233 | 7,526 | 7,408 | 8,708 | 7,035 | 6,065 | 5,976 | 6,290 | 6,772 | 6,645 | 8,068 | 5,956 | 4,191 | 4,119 |
| | 5 | 4,737 | 9,628 | 9,597 | 9,452 | 9,939 | 9,469 | 9,495 | 6,438 | 7,211 | 7,078 | 5,886 | 9,430 | 6,063 | 6,330 | 7,683 | 6,630 | 6,467 | 4,581 | 9,180 | 5,514 | 5,600 |
| | 6 | 5,299 | 9,628 | 9,585 | 9,512 | 9,691 | 9,904 | 9,491 | 5,925 | 7,517 | 6,794 | 5,812 | 7,386 | 8,749 | 5,763 | 6,485 | 6,466 | 5,974 | 4,190 | 6,505 | 7,983 | 4,239 |
| | 7 | 5,626 | 9,536 | 9,626 | 9,447 | 9,607 | 9,537 | 9,894 | 6,276 | 6,992 | 7,467 | 5,755 | 7,502 | 5,925 | 8,775 | 6,475 | 5,883 | 6,746 | 4,316 | 6,823 | 4,273 | 8,052 |

*0=(0,0,0), 1= (1,1,1), 2= (1,1,0), 3=(1,0,1), 4=(1,0,0), 5=(0,1,1), 6=(0,1,0), 7=(0,0,1)

$T^2$ chart. The results reveal significant performance advantages of the PoC approach:

(1) **Small Shift Detection**: The most substantial performance difference appears for small to moderate shifts. For $\delta = 0.25\sigma$, the $T^2$ chart's ARL values range from 82.27 to 89.76, while the PoC chart achieves ARL values between 5.47 and 5.88. This represents a detection speed improvement of approximately 15 times.

(2) **Correlation Impact**: The $T^2$ chart shows considerable sensitivity to correlation structures. For $\delta = 1.0\sigma$, the $T^2$ chart's ARL increases from 16.30 ($\rho_1 = 0.3$) to 27.05 ($\rho_3 = 0.8$), showing a 66% performance deterioration. In contrast, the PoC chart's ARL only increases from 3.28 to 4.25, representing a much smaller 30% change. This demonstrates the robust nature of the SVM-based approach across different correlation structures.

TABLE 4. 3. SVM-PoC (average values) calculated for $\Gamma_1$ from different combinations of changes

| Gamma_1 ( $\theta_1+\delta;\theta_2$ ) | | | | | | | | | | | | | | | | | | | | | | |
|---|---|---|---|---|---|---|---|---|---|---|---|---|---|---|---|---|---|---|---|---|---|---|
| | | $\rho_3=0,8$ | | | | | | | $\rho_2=0,5$ | | | | | | | $\rho_1=0,3$ | | | | | | |
| | | 1 | 2 | 3 | 4 | 5 | 6 | 7 | 1 | 2 | 3 | 4 | 5 | 6 | 7 | 1 | 2 | 3 | 4 | 5 | 6 | 7 |
| $\delta\sigma$ | 0 | 0,200 | 0,200 | 0,200 | 0,200 | 0,200 | 0,200 | 0,200 | 0,200 | 0,200 | 0,200 | 0,200 | 0,200 | 0,200 | 0,200 | 0,200 | 0,200 | 0,200 | 0,200 | 0,200 | 0,200 | 0,200 |
| | 1 | 0,236 | 0,220 | 0,221 | 0,207 | 0,218 | 0,205 | 0,205 | 0,236 | 0,220 | 0,221 | 0,207 | 0,218 | 0,205 | 0,205 | 0,246 | 0,220 | 0,226 | 0,207 | 0,222 | 0,207 | 0,206 |
| | 2 | 0,221 | 0,233 | 0,208 | 0,207 | 0,205 | 0,208 | 0,201 | 0,221 | 0,233 | 0,208 | 0,207 | 0,205 | 0,208 | 0,201 | 0,227 | 0,230 | 0,211 | 0,208 | 0,210 | 0,208 | 0,201 |
| | 3 | 0,224 | 0,208 | 0,231 | 0,208 | 0,208 | 0,201 | 0,207 | 0,224 | 0,208 | 0,231 | 0,208 | 0,208 | 0,201 | 0,207 | 0,227 | 0,211 | 0,231 | 0,209 | 0,210 | 0,201 | 0,208 |
| 0,5 | 4 | 0,211 | 0,212 | 0,212 | 0,218 | 0,202 | 0,201 | 0,200 | 0,211 | 0,212 | 0,212 | 0,218 | 0,202 | 0,201 | 0,200 | 0,214 | 0,214 | 0,212 | 0,212 | 0,204 | 0,201 | 0,201 |
| | 5 | 0,219 | 0,207 | 0,208 | 0,201 | 0,235 | 0,207 | 0,208 | 0,219 | 0,207 | 0,208 | 0,201 | 0,235 | 0,207 | 0,208 | 0,226 | 0,211 | 0,210 | 0,201 | 0,230 | 0,208 | 0,208 |
| | 6 | 0,208 | 0,213 | 0,202 | 0,200 | 0,211 | 0,219 | 0,200 | 0,208 | 0,213 | 0,202 | 0,200 | 0,211 | 0,219 | 0,200 | 0,213 | 0,212 | 0,203 | 0,201 | 0,212 | 0,212 | 0,201 |
| | 7 | 0,209 | 0,202 | 0,213 | 0,200 | 0,213 | 0,201 | 0,218 | 0,209 | 0,202 | 0,213 | 0,200 | 0,213 | 0,201 | 0,218 | 0,214 | 0,203 | 0,212 | 0,201 | 0,212 | 0,202 | 0,212 |
| | 1 | 0,332 | 0,275 | 0,272 | 0,225 | 0,274 | 0,224 | 0,222 | 0,332 | 0,275 | 0,272 | 0,225 | 0,274 | 0,224 | 0,222 | 0,377 | 0,287 | 0,291 | 0,224 | 0,290 | 0,223 | 0,225 |
| | 2 | 0,279 | 0,340 | 0,234 | 0,232 | 0,234 | 0,230 | 0,207 | 0,279 | 0,340 | 0,234 | 0,232 | 0,234 | 0,230 | 0,207 | 0,301 | 0,325 | 0,242 | 0,230 | 0,242 | 0,230 | 0,206 |
| | 3 | 0,280 | 0,236 | 0,340 | 0,230 | 0,237 | 0,207 | 0,231 | 0,280 | 0,236 | 0,340 | 0,230 | 0,237 | 0,207 | 0,231 | 0,296 | 0,242 | 0,324 | 0,229 | 0,243 | 0,208 | 0,229 |
| 1,0 | 4 | 0,226 | 0,234 | 0,236 | 0,292 | 0,208 | 0,202 | 0,202 | 0,226 | 0,234 | 0,236 | 0,292 | 0,208 | 0,202 | 0,202 | 0,236 | 0,237 | 0,236 | 0,260 | 0,212 | 0,203 | 0,202 |
| | 5 | 0,271 | 0,228 | 0,228 | 0,205 | 0,341 | 0,231 | 0,229 | 0,271 | 0,228 | 0,228 | 0,205 | 0,341 | 0,231 | 0,229 | 0,302 | 0,242 | 0,243 | 0,207 | 0,330 | 0,230 | 0,227 |
| | 6 | 0,224 | 0,233 | 0,210 | 0,203 | 0,234 | 0,286 | 0,203 | 0,224 | 0,233 | 0,210 | 0,203 | 0,234 | 0,286 | 0,203 | 0,234 | 0,234 | 0,213 | 0,203 | 0,235 | 0,259 | 0,203 |
| | 7 | 0,224 | 0,211 | 0,232 | 0,202 | 0,232 | 0,202 | 0,289 | 0,224 | 0,211 | 0,232 | 0,202 | 0,232 | 0,202 | 0,289 | 0,235 | 0,213 | 0,233 | 0,202 | 0,237 | 0,203 | 0,258 |
| | 1 | 0,462 | 0,353 | 0,360 | 0,256 | 0,355 | 0,250 | 0,252 | 0,462 | 0,353 | 0,360 | 0,256 | 0,355 | 0,250 | 0,252 | 0,550 | 0,390 | 0,392 | 0,249 | 0,384 | 0,250 | 0,249 |
| | 2 | 0,357 | 0,508 | 0,288 | 0,263 | 0,288 | 0,262 | 0,222 | 0,357 | 0,508 | 0,288 | 0,263 | 0,288 | 0,262 | 0,222 | 0,411 | 0,489 | 0,303 | 0,265 | 0,304 | 0,265 | 0,222 |
| | 3 | 0,363 | 0,295 | 0,490 | 0,268 | 0,303 | 0,228 | 0,266 | 0,363 | 0,295 | 0,490 | 0,268 | 0,303 | 0,228 | 0,266 | 0,418 | 0,315 | 0,477 | 0,264 | 0,308 | 0,222 | 0,262 |
| 1,5 | 4 | 0,259 | 0,277 | 0,279 | 0,400 | 0,240 | 0,210 | 0,210 | 0,259 | 0,277 | 0,279 | 0,400 | 0,240 | 0,210 | 0,210 | 0,268 | 0,275 | 0,273 | 0,339 | 0,235 | 0,208 | 0,207 |
| | 5 | 0,353 | 0,300 | 0,299 | 0,224 | 0,486 | 0,267 | 0,270 | 0,353 | 0,300 | 0,299 | 0,224 | 0,486 | 0,267 | 0,270 | 0,411 | 0,309 | 0,310 | 0,223 | 0,480 | 0,265 | 0,265 |
| | 6 | 0,261 | 0,275 | 0,234 | 0,209 | 0,276 | 0,409 | 0,208 | 0,261 | 0,275 | 0,234 | 0,209 | 0,276 | 0,409 | 0,208 | 0,268 | 0,270 | 0,238 | 0,208 | 0,269 | 0,342 | 0,209 |
| | 7 | 0,253 | 0,232 | 0,267 | 0,209 | 0,273 | 0,207 | 0,401 | 0,253 | 0,232 | 0,267 | 0,209 | 0,273 | 0,207 | 0,401 | 0,279 | 0,240 | 0,276 | 0,210 | 0,277 | 0,210 | 0,348 |
| | 1 | 0,602 | 0,447 | 0,455 | 0,280 | 0,451 | 0,277 | 0,286 | 0,602 | 0,447 | 0,455 | 0,280 | 0,451 | 0,277 | 0,286 | 0,695 | 0,470 | 0,477 | 0,271 | 0,484 | 0,283 | 0,277 |
| | 2 | 0,491 | 0,632 | 0,412 | 0,316 | 0,422 | 0,315 | 0,276 | 0,491 | 0,632 | 0,412 | 0,316 | 0,422 | 0,315 | 0,276 | 0,535 | 0,642 | 0,394 | 0,302 | 0,396 | 0,298 | 0,244 |
| | 3 | 0,476 | 0,397 | 0,655 | 0,309 | 0,397 | 0,258 | 0,313 | 0,476 | 0,397 | 0,655 | 0,309 | 0,397 | 0,258 | 0,313 | 0,544 | 0,410 | 0,632 | 0,302 | 0,404 | 0,251 | 0,306 |
| 2,0 | 4 | 0,330 | 0,344 | 0,341 | 0,522 | 0,294 | 0,230 | 0,227 | 0,330 | 0,344 | 0,341 | 0,522 | 0,294 | 0,230 | 0,227 | 0,338 | 0,338 | 0,344 | 0,448 | 0,288 | 0,222 | 0,221 |
| | 5 | 0,477 | 0,397 | 0,394 | 0,267 | 0,641 | 0,310 | 0,328 | 0,477 | 0,397 | 0,394 | 0,267 | 0,641 | 0,310 | 0,328 | 0,551 | 0,407 | 0,412 | 0,246 | 0,629 | 0,297 | 0,308 |
| | 6 | 0,338 | 0,345 | 0,295 | 0,232 | 0,341 | 0,525 | 0,229 | 0,338 | 0,345 | 0,295 | 0,232 | 0,341 | 0,525 | 0,229 | 0,324 | 0,333 | 0,278 | 0,218 | 0,324 | 0,445 | 0,219 |
| | 7 | 0,321 | 0,289 | 0,328 | 0,227 | 0,329 | 0,230 | 0,513 | 0,321 | 0,289 | 0,328 | 0,227 | 0,329 | 0,230 | 0,513 | 0,328 | 0,279 | 0,325 | 0,221 | 0,327 | 0,221 | 0,425 |
| | 1 | 0,705 | 0,548 | 0,544 | 0,339 | 0,542 | 0,341 | 0,337 | 0,705 | 0,548 | 0,544 | 0,339 | 0,542 | 0,341 | 0,337 | 0,793 | 0,565 | 0,561 | 0,305 | 0,548 | 0,306 | 0,307 |
| | 2 | 0,588 | 0,764 | 0,532 | 0,376 | 0,516 | 0,362 | 0,324 | 0,588 | 0,764 | 0,532 | 0,376 | 0,516 | 0,362 | 0,324 | 0,658 | 0,735 | 0,516 | 0,348 | 0,516 | 0,345 | 0,298 |
| | 3 | 0,574 | 0,511 | 0,768 | 0,360 | 0,512 | 0,334 | 0,358 | 0,574 | 0,511 | 0,768 | 0,360 | 0,512 | 0,334 | 0,358 | 0,654 | 0,502 | 0,744 | 0,348 | 0,506 | 0,288 | 0,338 |
| 2,5 | 4 | 0,431 | 0,440 | 0,435 | 0,624 | 0,394 | 0,273 | 0,274 | 0,431 | 0,440 | 0,435 | 0,624 | 0,394 | 0,273 | 0,274 | 0,420 | 0,395 | 0,406 | 0,548 | 0,357 | 0,239 | 0,244 |
| | 5 | 0,584 | 0,531 | 0,527 | 0,338 | 0,746 | 0,370 | 0,366 | 0,584 | 0,531 | 0,527 | 0,338 | 0,746 | 0,370 | 0,366 | 0,659 | 0,507 | 0,521 | 0,290 | 0,746 | 0,355 | 0,338 |
| | 6 | 0,437 | 0,436 | 0,404 | 0,275 | 0,436 | 0,635 | 0,269 | 0,437 | 0,436 | 0,404 | 0,275 | 0,436 | 0,635 | 0,269 | 0,430 | 0,409 | 0,365 | 0,242 | 0,423 | 0,553 | 0,245 |
| | 7 | 0,440 | 0,397 | 0,452 | 0,272 | 0,452 | 0,268 | 0,627 | 0,440 | 0,397 | 0,452 | 0,272 | 0,452 | 0,268 | 0,627 | 0,424 | 0,356 | 0,407 | 0,244 | 0,410 | 0,243 | 0,543 |
| | 1 | 0,789 | 0,599 | 0,602 | 0,373 | 0,594 | 0,372 | 0,372 | 0,789 | 0,599 | 0,602 | 0,373 | 0,594 | 0,372 | 0,372 | 0,863 | 0,630 | 0,642 | 0,337 | 0,624 | 0,323 | 0,338 |
| | 2 | 0,678 | 0,820 | 0,626 | 0,426 | 0,620 | 0,439 | 0,438 | 0,678 | 0,820 | 0,626 | 0,426 | 0,620 | 0,439 | 0,438 | 0,748 | 0,810 | 0,622 | 0,400 | 0,617 | 0,395 | 0,355 |
| | 3 | 0,684 | 0,625 | 0,836 | 0,439 | 0,620 | 0,422 | 0,437 | 0,684 | 0,625 | 0,836 | 0,439 | 0,620 | 0,422 | 0,437 | 0,752 | 0,620 | 0,809 | 0,402 | 0,633 | 0,369 | 0,393 |
| 3,0 | 4 | 0,540 | 0,539 | 0,529 | 0,711 | 0,511 | 0,345 | 0,359 | 0,540 | 0,539 | 0,529 | 0,711 | 0,511 | 0,345 | 0,359 | 0,514 | 0,500 | 0,494 | 0,632 | 0,454 | 0,289 | 0,281 |
| | 5 | 0,684 | 0,647 | 0,648 | 0,436 | 0,816 | 0,450 | 0,454 | 0,684 | 0,647 | 0,648 | 0,436 | 0,816 | 0,450 | 0,454 | 0,750 | 0,617 | 0,625 | 0,361 | 0,810 | 0,394 | 0,385 |
| | 6 | 0,542 | 0,545 | 0,519 | 0,349 | 0,550 | 0,715 | 0,348 | 0,542 | 0,545 | 0,519 | 0,349 | 0,550 | 0,715 | 0,348 | 0,516 | 0,495 | 0,455 | 0,281 | 0,502 | 0,629 | 0,281 |
| | 7 | 0,538 | 0,507 | 0,540 | 0,356 | 0,536 | 0,353 | 0,710 | 0,538 | 0,507 | 0,540 | 0,356 | 0,536 | 0,353 | 0,710 | 0,513 | 0,446 | 0,482 | 0,287 | 0,488 | 0,276 | 0,629 |

*0=(0,0,0), 1= (1,1,1), 2= (1,1,0), 3=(1,0,1), 4=(1,0,0), 5=(0,1,1), 6=(0,1,0), 7=(0,0,1)

(3) **Large Shift Performance**: Even for large shifts ($\delta \geq 2.5\sigma$), the PoC chart maintains its advantage, though the performance gap narrows. This is consistent with the known characteristics of Shewhart-type charts (including $T^2$), which become more effective for larger shifts.

The superior performance of the PoC chart can be attributed to the SVM's ability to establish a nonlinear decision boundary that better captures the complex relationships between variables, unlike the $T^2$ chart which relies on a quadratic form based on the inverse covariance matrix.

Table 4. 4. SVM-PoC (average values) calculated for $\Gamma_2$ from different combinations of changes

| | | Gamma_2 ( $\theta_1;\theta_2+\delta$ ) | | | | | | | | | | | | | | | | | | | | |
|---|---|---|---|---|---|---|---|---|---|---|---|---|---|---|---|---|---|---|---|---|---|---|
| | | $\rho_3=0,8$ | | | | | | | $\rho_2=0,5$ | | | | | | | $\rho_1=0,3$ | | | | | | |
| | | 1 | 2 | 3 | 4 | 5 | 6 | 7 | 1 | 2 | 3 | 4 | 5 | 6 | 7 | 1 | 2 | 3 | 4 | 5 | 6 | 7 |
| $\delta\sigma$ | 0 | 0,200 | 0,200 | 0,200 | 0,200 | 0,200 | 0,200 | 0,200 | 0,200 | 0,200 | 0,200 | 0,200 | 0,200 | 0,200 | 0,200 | 0,200 | 0,200 | 0,200 | 0,200 | 0,200 | 0,200 | 0,200 |
| | 1 | 0,208 | 0,207 | 0,206 | 0,203 | 0,207 | 0,202 | 0,202 | 0,211 | 0,205 | 0,206 | 0,202 | 0,204 | 0,203 | 0,202 | 0,216 | 0,206 | 0,206 | 0,203 | 0,205 | 0,202 | 0,203 |
| | 2 | 0,206 | 0,208 | 0,204 | 0,204 | 0,204 | 0,203 | 0,201 | 0,209 | 0,207 | 0,204 | 0,202 | 0,204 | 0,202 | 0,201 | 0,209 | 0,208 | 0,205 | 0,202 | 0,206 | 0,202 | 0,201 |
| | 3 | 0,207 | 0,204 | 0,210 | 0,204 | 0,206 | 0,201 | 0,203 | 0,209 | 0,206 | 0,208 | 0,202 | 0,205 | 0,201 | 0,202 | 0,212 | 0,205 | 0,209 | 0,203 | 0,206 | 0,201 | 0,203 |
| 0,5 | 4 | 0,205 | 0,205 | 0,205 | 0,205 | 0,202 | 0,201 | 0,200 | 0,207 | 0,204 | 0,204 | 0,204 | 0,202 | 0,201 | 0,201 | 0,206 | 0,205 | 0,205 | 0,205 | 0,204 | 0,201 | 0,201 |
| | 5 | 0,207 | 0,203 | 0,203 | 0,201 | 0,208 | 0,203 | 0,203 | 0,208 | 0,203 | 0,204 | 0,201 | 0,206 | 0,202 | 0,202 | 0,212 | 0,206 | 0,206 | 0,201 | 0,208 | 0,202 | 0,202 |
| | 6 | 0,205 | 0,206 | 0,201 | 0,201 | 0,205 | 0,204 | 0,200 | 0,206 | 0,204 | 0,202 | 0,201 | 0,205 | 0,204 | 0,201 | 0,208 | 0,204 | 0,203 | 0,201 | 0,205 | 0,203 | 0,201 |
| | 7 | 0,204 | 0,201 | 0,206 | 0,201 | 0,205 | 0,201 | 0,205 | 0,206 | 0,203 | 0,204 | 0,201 | 0,204 | 0,201 | 0,203 | 0,207 | 0,202 | 0,204 | 0,201 | 0,205 | 0,201 | 0,204 |
| | 1 | 0,230 | 0,217 | 0,218 | 0,209 | 0,222 | 0,209 | 0,210 | 0,239 | 0,223 | 0,223 | 0,209 | 0,221 | 0,209 | 0,210 | 0,250 | 0,223 | 0,224 | 0,209 | 0,226 | 0,210 | 0,210 |
| | 2 | 0,225 | 0,231 | 0,218 | 0,216 | 0,215 | 0,213 | 0,204 | 0,228 | 0,226 | 0,218 | 0,208 | 0,219 | 0,209 | 0,204 | 0,230 | 0,227 | 0,220 | 0,209 | 0,217 | 0,210 | 0,206 |
| | 3 | 0,225 | 0,214 | 0,229 | 0,215 | 0,215 | 0,204 | 0,213 | 0,230 | 0,214 | 0,225 | 0,210 | 0,216 | 0,204 | 0,208 | 0,233 | 0,218 | 0,229 | 0,209 | 0,220 | 0,205 | 0,209 |
| 1,0 | 4 | 0,216 | 0,215 | 0,215 | 0,217 | 0,205 | 0,202 | 0,203 | 0,217 | 0,213 | 0,213 | 0,211 | 0,206 | 0,203 | 0,202 | 0,220 | 0,212 | 0,212 | 0,212 | 0,208 | 0,204 | 0,202 |
| | 5 | 0,225 | 0,217 | 0,219 | 0,205 | 0,233 | 0,215 | 0,217 | 0,226 | 0,214 | 0,215 | 0,203 | 0,227 | 0,209 | 0,210 | 0,235 | 0,220 | 0,219 | 0,206 | 0,227 | 0,209 | 0,208 |
| | 6 | 0,216 | 0,221 | 0,207 | 0,203 | 0,219 | 0,227 | 0,203 | 0,218 | 0,213 | 0,207 | 0,203 | 0,215 | 0,210 | 0,203 | 0,220 | 0,215 | 0,209 | 0,203 | 0,215 | 0,212 | 0,203 |
| | 7 | 0,216 | 0,206 | 0,219 | 0,202 | 0,221 | 0,203 | 0,226 | 0,217 | 0,209 | 0,215 | 0,202 | 0,215 | 0,203 | 0,211 | 0,219 | 0,207 | 0,214 | 0,203 | 0,214 | 0,203 | 0,212 |
| | 1 | 0,251 | 0,238 | 0,242 | 0,219 | 0,240 | 0,219 | 0,222 | 0,265 | 0,243 | 0,245 | 0,218 | 0,241 | 0,217 | 0,218 | 0,294 | 0,252 | 0,253 | 0,221 | 0,242 | 0,220 | 0,221 |
| | 2 | 0,249 | 0,261 | 0,238 | 0,233 | 0,236 | 0,229 | 0,214 | 0,253 | 0,245 | 0,233 | 0,219 | 0,233 | 0,220 | 0,210 | 0,262 | 0,261 | 0,239 | 0,219 | 0,235 | 0,220 | 0,211 |
| | 3 | 0,246 | 0,232 | 0,259 | 0,227 | 0,231 | 0,210 | 0,231 | 0,250 | 0,233 | 0,247 | 0,219 | 0,231 | 0,208 | 0,220 | 0,269 | 0,241 | 0,260 | 0,220 | 0,241 | 0,213 | 0,220 |
| 1,5 | 4 | 0,230 | 0,238 | 0,235 | 0,256 | 0,215 | 0,207 | 0,206 | 0,228 | 0,224 | 0,220 | 0,220 | 0,212 | 0,205 | 0,205 | 0,229 | 0,225 | 0,223 | 0,224 | 0,217 | 0,207 | 0,205 |
| | 5 | 0,248 | 0,235 | 0,233 | 0,213 | 0,265 | 0,234 | 0,231 | 0,256 | 0,234 | 0,234 | 0,212 | 0,246 | 0,220 | 0,219 | 0,259 | 0,237 | 0,235 | 0,211 | 0,261 | 0,217 | 0,219 |
| | 6 | 0,229 | 0,237 | 0,215 | 0,207 | 0,233 | 0,249 | 0,207 | 0,228 | 0,224 | 0,213 | 0,205 | 0,223 | 0,221 | 0,206 | 0,236 | 0,229 | 0,217 | 0,206 | 0,228 | 0,221 | 0,207 |
| | 7 | 0,233 | 0,214 | 0,235 | 0,206 | 0,236 | 0,206 | 0,255 | 0,230 | 0,214 | 0,227 | 0,205 | 0,225 | 0,206 | 0,221 | 0,240 | 0,220 | 0,232 | 0,208 | 0,233 | 0,207 | 0,224 |
| | 1 | 0,282 | 0,269 | 0,268 | 0,241 | 0,268 | 0,240 | 0,236 | 0,307 | 0,263 | 0,267 | 0,234 | 0,261 | 0,232 | 0,232 | 0,328 | 0,276 | 0,275 | 0,235 | 0,279 | 0,232 | 0,225 |
| | 2 | 0,265 | 0,286 | 0,253 | 0,246 | 0,255 | 0,252 | 0,225 | 0,279 | 0,274 | 0,250 | 0,232 | 0,252 | 0,230 | 0,218 | 0,295 | 0,289 | 0,263 | 0,227 | 0,263 | 0,235 | 0,220 |
| | 3 | 0,279 | 0,257 | 0,297 | 0,251 | 0,259 | 0,225 | 0,256 | 0,285 | 0,255 | 0,268 | 0,233 | 0,255 | 0,218 | 0,229 | 0,298 | 0,264 | 0,284 | 0,231 | 0,261 | 0,223 | 0,233 |
| 2,0 | 4 | 0,247 | 0,259 | 0,258 | 0,290 | 0,226 | 0,212 | 0,211 | 0,242 | 0,237 | 0,238 | 0,235 | 0,221 | 0,208 | 0,208 | 0,253 | 0,240 | 0,237 | 0,236 | 0,224 | 0,209 | 0,211 |
| | 5 | 0,274 | 0,258 | 0,258 | 0,226 | 0,291 | 0,251 | 0,254 | 0,278 | 0,250 | 0,249 | 0,218 | 0,272 | 0,229 | 0,231 | 0,301 | 0,264 | 0,268 | 0,221 | 0,290 | 0,233 | 0,235 |
| | 6 | 0,246 | 0,260 | 0,230 | 0,213 | 0,257 | 0,288 | 0,216 | 0,247 | 0,235 | 0,223 | 0,209 | 0,235 | 0,234 | 0,208 | 0,256 | 0,242 | 0,230 | 0,212 | 0,242 | 0,236 | 0,211 |
| | 7 | 0,248 | 0,226 | 0,256 | 0,212 | 0,251 | 0,213 | 0,283 | 0,247 | 0,225 | 0,240 | 0,209 | 0,239 | 0,209 | 0,234 | 0,250 | 0,228 | 0,241 | 0,209 | 0,237 | 0,209 | 0,238 |
| | 1 | 0,306 | 0,286 | 0,288 | 0,254 | 0,276 | 0,251 | 0,252 | 0,326 | 0,289 | 0,283 | 0,241 | 0,285 | 0,240 | 0,240 | 0,359 | 0,308 | 0,297 | 0,246 | 0,298 | 0,245 | 0,246 |
| | 2 | 0,299 | 0,325 | 0,279 | 0,273 | 0,285 | 0,281 | 0,238 | 0,320 | 0,299 | 0,285 | 0,249 | 0,280 | 0,240 | 0,227 | 0,337 | 0,314 | 0,299 | 0,247 | 0,290 | 0,236 | 0,234 |
| | 3 | 0,294 | 0,288 | 0,348 | 0,286 | 0,290 | 0,244 | 0,287 | 0,296 | 0,268 | 0,288 | 0,241 | 0,268 | 0,223 | 0,241 | 0,328 | 0,288 | 0,309 | 0,241 | 0,280 | 0,229 | 0,243 |
| 2,5 | 4 | 0,274 | 0,281 | 0,285 | 0,317 | 0,252 | 0,228 | 0,227 | 0,264 | 0,254 | 0,249 | 0,250 | 0,235 | 0,214 | 0,214 | 0,271 | 0,254 | 0,257 | 0,249 | 0,239 | 0,215 | 0,216 |
| | 5 | 0,302 | 0,288 | 0,288 | 0,243 | 0,332 | 0,275 | 0,280 | 0,311 | 0,273 | 0,274 | 0,228 | 0,292 | 0,242 | 0,242 | 0,330 | 0,288 | 0,288 | 0,232 | 0,313 | 0,245 | 0,242 |
| | 6 | 0,266 | 0,277 | 0,240 | 0,224 | 0,276 | 0,315 | 0,222 | 0,252 | 0,244 | 0,228 | 0,211 | 0,244 | 0,247 | 0,212 | 0,261 | 0,251 | 0,234 | 0,214 | 0,248 | 0,248 | 0,213 |
| | 7 | 0,278 | 0,255 | 0,292 | 0,225 | 0,288 | 0,228 | 0,320 | 0,253 | 0,229 | 0,247 | 0,212 | 0,241 | 0,212 | 0,242 | 0,271 | 0,240 | 0,253 | 0,218 | 0,254 | 0,217 | 0,252 |
| | 1 | 0,317 | 0,294 | 0,290 | 0,262 | 0,296 | 0,255 | 0,256 | 0,349 | 0,314 | 0,297 | 0,255 | 0,314 | 0,255 | 0,258 | 0,405 | 0,329 | 0,332 | 0,251 | 0,329 | 0,251 | 0,257 |
| | 2 | 0,311 | 0,347 | 0,300 | 0,288 | 0,294 | 0,289 | 0,254 | 0,334 | 0,318 | 0,293 | 0,258 | 0,295 | 0,258 | 0,237 | 0,369 | 0,342 | 0,312 | 0,263 | 0,316 | 0,263 | 0,241 |
| | 3 | 0,308 | 0,301 | 0,356 | 0,297 | 0,308 | 0,258 | 0,297 | 0,307 | 0,279 | 0,315 | 0,246 | 0,275 | 0,231 | 0,246 | 0,369 | 0,320 | 0,348 | 0,262 | 0,324 | 0,244 | 0,263 |
| 3,0 | 4 | 0,268 | 0,281 | 0,281 | 0,321 | 0,251 | 0,226 | 0,227 | 0,272 | 0,265 | 0,264 | 0,260 | 0,243 | 0,217 | 0,219 | 0,281 | 0,268 | 0,260 | 0,265 | 0,248 | 0,220 | 0,220 |
| | 5 | 0,311 | 0,292 | 0,292 | 0,251 | 0,340 | 0,282 | 0,289 | 0,338 | 0,297 | 0,299 | 0,240 | 0,323 | 0,263 | 0,262 | 0,363 | 0,316 | 0,313 | 0,243 | 0,350 | 0,259 | 0,263 |
| | 6 | 0,291 | 0,302 | 0,269 | 0,241 | 0,307 | 0,345 | 0,238 | 0,279 | 0,266 | 0,243 | 0,218 | 0,265 | 0,265 | 0,220 | 0,287 | 0,268 | 0,251 | 0,221 | 0,266 | 0,265 | 0,222 |
| | 7 | 0,298 | 0,273 | 0,301 | 0,237 | 0,310 | 0,239 | 0,346 | 0,274 | 0,248 | 0,264 | 0,220 | 0,266 | 0,218 | 0,263 | 0,297 | 0,255 | 0,273 | 0,222 | 0,272 | 0,222 | 0,266 |

*0=(0,0,0), 1= (1,1,1), 2= (1,1,0), 3=(1,0,1), 4=(1,0,0), 5=(0,1,1), 6=(0,1,0), 7=(0,0,1)

### Multivariate Non-Normal (Gamma) Distribution Processes

*i. Shift Detection Performance.* Table 3 presents ARL values for the PoC chart under three different gamma distribution scenarios, each representing a different parameter shift:

(1) **Gamma$_1$ (Scale Parameter Shift)**: When shifts occur in the scale parameter, the PoC chart demonstrates excellent performance even for small shifts ($\delta = 0.25$), with ARL values ranging from 1.88 to 5.78 depending on correlation structure. For shifts of $\delta \geq 0.5$, the ARL values drop below 2, indicating nearly immediate detection.

TABLE 4. 5. SVM-PoC (average values) in $\Gamma_3$ obtained from different combinations of changes

| | | Gamma_3( $\theta_1+\delta;\theta_2+\delta$ ) | | | | | | | | | | | | | | | | | | | | |
|---|---|---|---|---|---|---|---|---|---|---|---|---|---|---|---|---|---|---|---|---|---|---|
| | | $\rho_3=0{,}8$ | | | | | | | $\rho_2=0{,}5$ | | | | | | | $\rho_1=0{,}3$ | | | | | | |
| $\delta$ | | 1 | 2 | 3 | 4 | 5 | 6 | 7 | 1 | 2 | 3 | 4 | 5 | 6 | 7 | 1 | 2 | 3 | 4 | 5 | 6 | 7 |
| 0 | 0 | 0,200 | 0,200 | 0,200 | 0,200 | 0,200 | 0,200 | 0,200 | 0,200 | 0,200 | 0,200 | 0,200 | 0,200 | 0,200 | 0,200 | 0,200 | 0,200 | 0,200 | 0,200 | 0,200 | 0,200 | 0,200 |
| | 1 | 0,298 | 0,293 | 0,295 | 0,252 | 0,297 | 0,253 | 0,257 | 0,337 | 0,301 | 0,297 | 0,241 | 0,297 | 0,239 | 0,239 | 0,394 | 0,326 | 0,323 | 0,246 | 0,324 | 0,247 | 0,243 |
| | 2 | 0,288 | 0,442 | 0,287 | 0,293 | 0,289 | 0,292 | 0,246 | 0,302 | 0,322 | 0,263 | 0,246 | 0,262 | 0,247 | 0,220 | 0,328 | 0,328 | 0,273 | 0,242 | 0,275 | 0,246 | 0,220 |
| | 3 | 0,291 | 0,289 | 0,445 | 0,288 | 0,295 | 0,247 | 0,291 | 0,304 | 0,263 | 0,325 | 0,244 | 0,262 | 0,218 | 0,246 | 0,328 | 0,276 | 0,325 | 0,243 | 0,275 | 0,222 | 0,246 |
| 0,5 | 4 | 0,251 | 0,289 | 0,292 | 0,449 | 0,247 | 0,224 | 0,223 | 0,245 | 0,248 | 0,251 | 0,286 | 0,223 | 0,207 | 0,208 | 0,253 | 0,250 | 0,252 | 0,261 | 0,226 | 0,208 | 0,209 |
| | 5 | 0,290 | 0,290 | 0,290 | 0,251 | 0,453 | 0,301 | 0,301 | 0,308 | 0,264 | 0,263 | 0,219 | 0,329 | 0,245 | 0,248 | 0,335 | 0,279 | 0,275 | 0,222 | 0,327 | 0,246 | 0,243 |
| | 6 | 0,255 | 0,287 | 0,248 | 0,225 | 0,286 | 0,450 | 0,225 | 0,247 | 0,247 | 0,224 | 0,209 | 0,246 | 0,279 | 0,208 | 0,256 | 0,247 | 0,226 | 0,208 | 0,249 | 0,264 | 0,208 |
| | 7 | 0,254 | 0,250 | 0,294 | 0,224 | 0,298 | 0,227 | 0,455 | 0,246 | 0,223 | 0,249 | 0,207 | 0,247 | 0,207 | 0,287 | 0,252 | 0,226 | 0,250 | 0,208 | 0,249 | 0,209 | 0,260 |
| | 1 | 0,626 | 0,614 | 0,614 | 0,550 | 0,617 | 0,549 | 0,555 | 0,676 | 0,620 | 0,619 | 0,454 | 0,615 | 0,452 | 0,454 | 0,769 | 0,664 | 0,661 | 0,449 | 0,662 | 0,441 | 0,444 |
| | 2 | 0,574 | 0,830 | 0,694 | 0,677 | 0,691 | 0,673 | 0,637 | 0,626 | 0,663 | 0,579 | 0,463 | 0,576 | 0,468 | 0,432 | 0,681 | 0,667 | 0,603 | 0,448 | 0,599 | 0,449 | 0,421 |
| | 3 | 0,620 | 0,688 | 0,827 | 0,670 | 0,690 | 0,634 | 0,667 | 0,621 | 0,573 | 0,669 | 0,471 | 0,579 | 0,433 | 0,469 | 0,696 | 0,616 | 0,687 | 0,455 | 0,607 | 0,415 | 0,450 |
| 1,0 | 4 | 0,593 | 0,667 | 0,674 | 0,823 | 0,646 | 0,590 | 0,597 | 0,488 | 0,472 | 0,475 | 0,565 | 0,457 | 0,346 | 0,340 | 0,490 | 0,455 | 0,450 | 0,499 | 0,447 | 0,315 | 0,315 |
| | 5 | 0,625 | 0,692 | 0,698 | 0,635 | 0,832 | 0,680 | 0,681 | 0,632 | 0,580 | 0,586 | 0,438 | 0,680 | 0,471 | 0,465 | 0,684 | 0,605 | 0,606 | 0,419 | 0,672 | 0,447 | 0,448 |
| | 6 | 0,591 | 0,669 | 0,639 | 0,596 | 0,669 | 0,820 | 0,587 | 0,477 | 0,467 | 0,448 | 0,334 | 0,463 | 0,555 | 0,341 | 0,476 | 0,453 | 0,429 | 0,313 | 0,453 | 0,493 | 0,316 |
| | 7 | 0,578 | 0,628 | 0,655 | 0,586 | 0,655 | 0,578 | 0,809 | 0,486 | 0,454 | 0,471 | 0,343 | 0,478 | 0,340 | 0,572 | 0,468 | 0,426 | 0,441 | 0,309 | 0,441 | 0,308 | 0,493 |
| | 1 | 0,833 | 0,843 | 0,841 | 0,811 | 0,844 | 0,814 | 0,813 | 0,887 | 0,848 | 0,848 | 0,703 | 0,846 | 0,690 | 0,702 | 0,933 | 0,865 | 0,860 | 0,654 | 0,867 | 0,658 | 0,657 |
| | 2 | 0,811 | 0,947 | 0,881 | 0,881 | 0,882 | 0,892 | 0,859 | 0,852 | 0,875 | 0,828 | 0,719 | 0,828 | 0,720 | 0,716 | 0,898 | 0,891 | 0,847 | 0,683 | 0,851 | 0,688 | 0,676 |
| | 3 | 0,830 | 0,877 | 0,946 | 0,884 | 0,878 | 0,858 | 0,881 | 0,856 | 0,833 | 0,882 | 0,725 | 0,834 | 0,716 | 0,720 | 0,884 | 0,847 | 0,876 | 0,683 | 0,841 | 0,674 | 0,678 |
| 1,5 | 4 | 0,802 | 0,858 | 0,860 | 0,934 | 0,836 | 0,826 | 0,827 | 0,734 | 0,720 | 0,722 | 0,781 | 0,711 | 0,616 | 0,619 | 0,740 | 0,717 | 0,717 | 0,740 | 0,722 | 0,572 | 0,573 |
| | 5 | 0,830 | 0,878 | 0,879 | 0,853 | 0,946 | 0,893 | 0,883 | 0,857 | 0,836 | 0,836 | 0,720 | 0,887 | 0,728 | 0,728 | 0,896 | 0,852 | 0,852 | 0,679 | 0,891 | 0,690 | 0,683 |
| | 6 | 0,803 | 0,867 | 0,845 | 0,836 | 0,865 | 0,939 | 0,829 | 0,745 | 0,732 | 0,728 | 0,626 | 0,733 | 0,785 | 0,630 | 0,718 | 0,697 | 0,695 | 0,565 | 0,697 | 0,719 | 0,561 |
| | 7 | 0,800 | 0,835 | 0,862 | 0,828 | 0,856 | 0,831 | 0,931 | 0,730 | 0,709 | 0,713 | 0,613 | 0,717 | 0,613 | 0,774 | 0,724 | 0,703 | 0,712 | 0,570 | 0,704 | 0,567 | 0,727 |
| | 1 | 0,925 | 0,938 | 0,936 | 0,921 | 0,934 | 0,921 | 0,922 | 0,964 | 0,941 | 0,942 | 0,853 | 0,937 | 0,851 | 0,848 | 0,984 | 0,948 | 0,951 | 0,799 | 0,951 | 0,802 | 0,810 |
| | 2 | 0,922 | 0,978 | 0,942 | 0,949 | 0,944 | 0,948 | 0,933 | 0,944 | 0,956 | 0,938 | 0,871 | 0,935 | 0,862 | 0,872 | 0,967 | 0,964 | 0,949 | 0,835 | 0,952 | 0,838 | 0,849 |
| | 3 | 0,924 | 0,948 | 0,979 | 0,953 | 0,947 | 0,935 | 0,955 | 0,950 | 0,940 | 0,965 | 0,880 | 0,940 | 0,880 | 0,879 | 0,960 | 0,945 | 0,958 | 0,836 | 0,947 | 0,850 | 0,835 |
| 2,0 | 4 | 0,900 | 0,931 | 0,934 | 0,969 | 0,911 | 0,917 | 0,916 | 0,874 | 0,871 | 0,866 | 0,895 | 0,864 | 0,812 | 0,808 | 0,846 | 0,836 | 0,833 | 0,854 | 0,839 | 0,755 | 0,764 |
| | 5 | 0,928 | 0,951 | 0,954 | 0,943 | 0,984 | 0,959 | 0,961 | 0,948 | 0,939 | 0,940 | 0,876 | 0,960 | 0,873 | 0,873 | 0,970 | 0,951 | 0,951 | 0,850 | 0,964 | 0,833 | 0,832 |
| | 6 | 0,899 | 0,931 | 0,916 | 0,922 | 0,933 | 0,969 | 0,916 | 0,870 | 0,860 | 0,859 | 0,803 | 0,856 | 0,890 | 0,798 | 0,856 | 0,849 | 0,856 | 0,777 | 0,851 | 0,860 | 0,766 |
| | 7 | 0,891 | 0,905 | 0,925 | 0,910 | 0,925 | 0,908 | 0,968 | 0,881 | 0,868 | 0,871 | 0,811 | 0,873 | 0,809 | 0,902 | 0,859 | 0,852 | 0,850 | 0,768 | 0,849 | 0,770 | 0,856 |
| | 1 | 0,971 | 0,975 | 0,976 | 0,969 | 0,974 | 0,969 | 0,967 | 0,989 | 0,979 | 0,978 | 0,935 | 0,979 | 0,929 | 0,936 | 0,996 | 0,985 | 0,984 | 0,912 | 0,984 | 0,908 | 0,906 |
| | 2 | 0,968 | 0,991 | 0,974 | 0,978 | 0,976 | 0,980 | 0,972 | 0,983 | 0,984 | 0,975 | 0,946 | 0,975 | 0,942 | 0,947 | 0,990 | 0,988 | 0,984 | 0,920 | 0,982 | 0,924 | 0,925 |
| | 3 | 0,965 | 0,974 | 0,984 | 0,978 | 0,975 | 0,972 | 0,975 | 0,981 | 0,974 | 0,983 | 0,938 | 0,972 | 0,931 | 0,944 | 0,990 | 0,982 | 0,985 | 0,923 | 0,982 | 0,926 | 0,921 |
| 2,5 | 4 | 0,946 | 0,964 | 0,964 | 0,986 | 0,951 | 0,959 | 0,953 | 0,933 | 0,930 | 0,925 | 0,949 | 0,931 | 0,890 | 0,891 | 0,933 | 0,924 | 0,922 | 0,932 | 0,925 | 0,879 | 0,879 |
| | 5 | 0,965 | 0,976 | 0,978 | 0,971 | 0,992 | 0,980 | 0,980 | 0,983 | 0,979 | 0,976 | 0,940 | 0,987 | 0,934 | 0,946 | 0,989 | 0,982 | 0,983 | 0,926 | 0,985 | 0,921 | 0,923 |
| | 6 | 0,945 | 0,966 | 0,947 | 0,952 | 0,964 | 0,984 | 0,956 | 0,935 | 0,934 | 0,930 | 0,898 | 0,928 | 0,945 | 0,896 | 0,929 | 0,927 | 0,930 | 0,882 | 0,924 | 0,936 | 0,885 |
| | 7 | 0,941 | 0,950 | 0,963 | 0,952 | 0,963 | 0,955 | 0,983 | 0,942 | 0,938 | 0,937 | 0,908 | 0,935 | 0,903 | 0,948 | 0,937 | 0,928 | 0,925 | 0,885 | 0,927 | 0,882 | 0,934 |
| | 1 | 0,989 | 0,989 | 0,987 | 0,987 | 0,990 | 0,985 | 0,987 | 0,997 | 0,993 | 0,992 | 0,974 | 0,993 | 0,972 | 0,974 | 0,999 | 0,994 | 0,995 | 0,962 | 0,994 | 0,959 | 0,959 |
| | 2 | 0,987 | 0,994 | 0,989 | 0,990 | 0,989 | 0,989 | 0,988 | 0,992 | 0,995 | 0,990 | 0,976 | 0,990 | 0,973 | 0,975 | 0,998 | 0,995 | 0,993 | 0,965 | 0,993 | 0,963 | 0,954 |
| | 3 | 0,986 | 0,987 | 0,990 | 0,989 | 0,988 | 0,987 | 0,990 | 0,994 | 0,992 | 0,995 | 0,977 | 0,992 | 0,968 | 0,963 | 0,998 | 0,993 | 0,996 | 0,967 | 0,994 | 0,958 | 0,969 |
| 3,0 | 4 | 0,966 | 0,980 | 0,979 | 0,991 | 0,968 | 0,973 | 0,975 | 0,976 | 0,971 | 0,968 | 0,979 | 0,971 | 0,952 | 0,951 | 0,964 | 0,960 | 0,958 | 0,974 | 0,962 | 0,934 | 0,935 |
| | 5 | 0,985 | 0,989 | 0,989 | 0,988 | 0,993 | 0,987 | 0,986 | 0,993 | 0,991 | 0,990 | 0,971 | 0,995 | 0,976 | 0,977 | 0,958 | 0,994 | 0,994 | 0,954 | 0,996 | 0,963 | 0,965 |
| | 6 | 0,966 | 0,977 | 0,967 | 0,971 | 0,984 | 0,991 | 0,976 | 0,973 | 0,967 | 0,965 | 0,943 | 0,965 | 0,979 | 0,945 | 0,963 | 0,962 | 0,961 | 0,934 | 0,961 | 0,974 | 0,934 |
| | 7 | 0,964 | 0,966 | 0,977 | 0,977 | 0,979 | 0,977 | 0,991 | 0,966 | 0,960 | 0,964 | 0,936 | 0,964 | 0,939 | 0,979 | 0,964 | 0,963 | 0,957 | 0,932 | 0,958 | 0,933 | 0,971 |

*0=(0,0,0), 1= (1,1,1), 2= (1,1,0), 3=(1,0,1), 4=(1,0,0), 5=(0,1,1), 6=(0,1,0), 7=(0,0,1)

(2) **Gamma$_2$ (Shape Parameter Shift)**: For shape parameter shifts, the chart shows even greater sensitivity, with ARL values for $\delta = 0.25$ between 1.50 and 2.02. This high sensitivity persists across all correlation structures, though with a slight efficiency decrease as correlation increases.

(3) **Gamma$_3$ (Both Parameters Shift)**: The most remarkable performance is observed when both shape and scale parameters shift simultaneously. For $\delta = 0.25$, ARL values range from 1.33 to 1.53, and for shifts of $\delta \geq 0.5$, detection is almost immediate with ARL values very close to 1.

Comparing across the three gamma scenarios, the PoC chart shows the highest sensitivity to shifts affecting both parameters (Gamma$_3$), followed by shape parameter shifts (Gamma$_2$), and then scale parameter shifts (Gamma$_1$). This pattern aligns with statistical theory, as simultaneous changes in both parameters create more substantial distributional changes that are easier to detect.

*ii. Correlation Effects in Non-Normal Distributions.* Unlike many traditional control charts, the PoC chart maintains robust performance across different correlation structures even in non-normal distributions. For the $\text{Gamma}_1$ scenario at $\delta = 0.25$, the ARL decreases from 5.78 ($\rho_3 = 0.8$) to 1.88 ($\rho_1 = 0.3$), showing that lower correlation enhances detection capability. This trend is consistent across all three gamma scenarios, though less pronounced in $\text{Gamma}_3$.

Compared to existing methods for non-normal distributions (such as those based on rank transformations or empirical likelihood), the PoC approach offers significant advantages in terms of detection speed and correlation robustness. Many traditional approaches for non-normal distributions suffer from decreased sensitivity or increased computational complexity, whereas the SVM-based method maintains high performance without distribution-specific adjustments.

### Interpretation in the Context of Existing Methods

The remarkable performance of the SVM-PoC approach can be understood through several methodological advantages:

(1) **Distribution-Free Nature**: Unlike parametric methods that rely on specific distribution assumptions, the SVM approach makes minimal assumptions about the underlying distribution, allowing it to perform well across normal and non-normal scenarios.

(2) **Optimal Separation Boundary**: The SVM's kernel-based approach enables the identification of complex, non-linear separation boundaries between in-control and out-of-control states, providing greater detection power than methods based on linear or quadratic forms.

(3) **Dimension Handling**: Traditional methods often struggle with the "curse of dimensionality" and correlation structures. The SVM approach effectively handles these challenges through its margin-based classification approach.

(4) **Robustness to Parameter Estimation**: The SVM method appears less sensitive to estimation errors in process parameters compared to traditional approaches like $T^2$, which can be heavily influenced by errors in estimating the covariance matrix.

When compared to other advanced MSPC methods such as MEWMA (Multivariate Exponentially Weighted Moving Average) or MCUSUM (Multivariate Cumulative Sum), which are known for their sensitivity to small shifts, the PoC approach demonstrates competitive or superior performance without requiring the specification of additional parameters (like smoothing constants) or assuming specific shift patterns.

These results position the SVM-PoC method as a powerful, flexible alternative to traditional MSPC techniques, particularly valuable in industrial settings where non-normality and complex variable relationships are common.

## 6. **Conclusion**

This study aimed to develop an advanced method for multivariate statistical process control (MSPC) that addresses two critical challenges: detecting shifts in process parameters and identifying the variables responsible for these shifts. Our proposed approach, based on Support Vector Machines (SVM) and the Probability of Control (PoC) concept, offers a robust solution for both normally distributed and non-normal multivariate processes.

*Key Findings and Implications,*

*Superior Performance in Shift Detection:* The SVM-PoC control chart consistently outperformed traditional methods, such as Hotelling's $T^2$ chart, especially in detecting small shifts. This improvement is particularly noteworthy given that Shewhart-type control charts, including $T^2$, are known for their limitations in capturing small process shifts due to their memoryless nature.

*Robustness to Non-Normality:* Our method demonstrated excellent performance across various scenarios of multivariate gamma-distributed processes. The PoC control chart effectively detected shifts in shape parameters ($\text{Gamma}_1$), scale parameters ($\text{Gamma}_2$), and combined shifts ($\text{Gamma}_3$), even for small shift magnitudes ($\delta \geq 0.25$).

*Insensitivity to Correlation Structures:* Unlike traditional methods whose performance degrades with increasing correlation between variables, the SVM-PoC approach maintained its effectiveness across low, medium, and high correlation levels. This feature makes it particularly valuable for real-world processes where variable interdependencies are common.

*Accurate Source Identification:* The proposed method accurately identified the variables responsible for process shifts in both normal and non-normal distributions, even for relatively small shifts ($\delta \geq 0.5\sigma$). This capability addresses a significant gap in many existing MSPC techniques and provides crucial information for process improvement efforts.

*Flexibility and Wide Applicability:* By demonstrating effectiveness in both normal and non-normal distributions, our method offers a versatile tool for a wide range of industrial processes. This flexibility eliminates the need for practitioners to switch between different control charts based on distributional assumptions.

*Early Detection:* The SVM-PoC control chart's ability to detect shifts earlier than traditional methods translates to faster response times in industrial settings, potentially reducing waste, improving quality, and increasing overall process efficiency.

*Future Research and Improvement,*

*Variance-Covariance Shifts:* The current method focuses primarily on shifts in mean vectors. Future work could extend the approach to detect shifts in the variance-covariance matrix or simultaneous shifts in both mean and variance-covariance parameters.

*Other Non-Normal Distributions:* While we demonstrated effectiveness with gamma distributions, further studies could explore the method's performance with other non-normal distributions common in industrial processes.

*Real-World Application:* Although our simulation studies provide strong evidence of the method's effectiveness, implementing and testing the approach in real industrial settings would provide valuable insights and potentially reveal areas for further refinement.

*Computational Efficiency:* As processes become more complex with higher dimensionality, optimizing the computational efficiency of the SVM-PoC approach could be an important area for future work.

In conclusion, the proposed SVM-PoC method represents a significant advancement in multivariate statistical process control. By addressing the dual challenges of shift detection and source identification across various process conditions, it offers a powerful tool for process monitoring and improvement in modern manufacturing and service industries. Its robustness to non-normality and correlation structures, combined with its accuracy in identifying shift sources, positions it as a valuable addition to the MSPC toolkit, capable of enhancing process quality and efficiency across a wide range of applications.

## REFERENCES

[1] *Y. Zhao, S. Wang, and J. Xiao*, A deep learning approach for multivariate statistical process monitoring and fault diagnosis, Expert Systems with Applications, **213**(2023), 118917.

[2] *Z. Li, H. Fang, and K. Peng*, Multivariate statistical process monitoring based on variational autoencoder and Gaussian mixture model, IEEE Transactions on Industrial Informatics, **18**(2022), No. 7, 4708–4718.

[3] *R. Y. Liu*, Control charts for multivariate processes, Journal of the American Statistical Association, **90**(1995), 1380–1387.

[4] *J. V. Kresta, J. F. MacGregor, and T. E. Marlin*, Multivariate statistical monitoring of process operating performance, Canadian Journal of Chemical Engineering, **69**(1991), No. 1, 35–47.

[5] *J. E. Jackson*, Principal Components and Factor Analysis: Part I Principal Components, Journal of Quality Technology, **12**(1980), No. 4, 201–213.

[6] *K. Wang, J. Zhu, and W. Wang*, Multivariate process monitoring using deep transfer learning and multitask learning, IEEE Transactions on Industrial Informatics, **19**(2023), No. 5, 6229–6239.

[7] *H. Hotelling*, Multivariate Quality Control, in Techniques of Statistical Analysis, C. Eisenhart, M. W. Hastay, and W. A. Wallis, Eds., McGraw-Hill, 1947.

[8] *C. A. Lowry, W. H. Woodall, C. W. Champ, and S. E. Rigdon*, A multivariate exponentially weighted moving average control chart, Technometrics, **34**(1992), No. 1, 46.

[9] *Y. S. Chang and D. S. Bai*, A multivariate T2 control chart for skewed populations using weighted standard deviations, Quality and Reliability Engineering International, **20**(2004), 31–46.

[10] *A. Khormali and J. Addeh*, A novel approach for recognition of control chart patterns: Type-2 fuzzy clustering optimized support vector machine, ISA Transactions, **109**(2021), 265–279.

[11] *Q. Jiang, X. Yan, and B. Huang*, Review and perspective on data-driven root cause diagnosis, Annual Reviews in Control, **53**(2022), 181–198.

[12] *Y. Yao and F. Gao*, A review of multistage process monitoring methods, Industrial & Engineering Chemistry Research, **61**(2022), No. 1, 4–29.

[13] *C. Shang, B. Huang, and F. You*, Data analytics and machine learning for smart manufacturing: Recent advances and perspectives, Engineering, **9**(2023), No. 3, 312–335.

[14] *H. Wu, J. Zhao, and W. Chen*, A review of process monitoring and fault diagnosis in wind turbines, Applied Energy, **281**(2021), 116108.

[15] *Y. Liao, X. Zeng, and W. Li*, Wavelet transform-based convolutional neural network for gearbox fault classification, Journal of Intelligent Manufacturing, **34**(2023), No. 2, 1–16.

[16] *O. Janssens, B. Vervisch, K. Stockman, and M. Loccufier*, Convolutional neural network-based fault detection for rotating machinery, Journal of Sound and Vibration, **489**(2023), 115682.

[17] *Z. Ge, Z. Song, and B. Huang*, Review of recent research on data-based process monitoring, Industrial & Engineering Chemistry Research, **60**(2021), No. 13, 4641–4663.

[18] *H. B. Bisheh and G. G. Amiri*, Structural damage detection based on variational mode decomposition and kernel PCA-based support vector machine, Engineering Structures, **278**(2023), 1–12.

[19] *J. Yu*, Machine learning in statistical process monitoring: A comprehensive review, Journal of Process Control, **110**(2022), 79–102.

[20] *P. Chongfuangprinya, S. B. Kim, S.-K. Park, and T. Sukchotrat*, Integration of support vector machines and control charts for multivariate process monitoring, Journal of Statistical Computation and Simulation, **81**(2011), No. 9, 1157–1173.